Weierstraß-Institut
für Angewandte Analysis und Stochastik

im Forschungsverbund Berlin e.V.

Preprint ISSN 0946 – 8633

High-Frequency Pulsations in DFB-Lasers with Amplified Feedback

Olaf Brox[1], Stefan Bauer[1], Mindaugas Radziunas[2], Matthias Wolfrum[2], Jan Sieber[3], Jochen Kreissl[1], Bernd Sartorius[1], and Hans-Jürgen Wünsche[4,1]

submitted: 22nd May 2003

[1] Fraunhofer-Institut für Nachrichtentechnik
Heinrich-Hertz-Institut
Einsteinufer 37
D – 10587 Berlin
Germany
E-Mail: brox@hhi.de, bauer@hhi.de, kreissl@hhi.de, sartorius@hhi.de

[2] Weierstraß-Institut
für Angewandte Analysis und Stochastik
Mohrenstrasse 39
D – 10117 Berlin
Germany
E-Mail: radziuna@wias-berlin.de, wolfrum@wias-berlin.de

[3] Dept. of Engineering Mathematics
University of Bristol
Bristol BS8 1TR
United Kingdom
E-Mail: Jan.Sieber@bristol.ac.uk

[4] Humboldt-Universität zu Berlin
Institut für Physik
Invalidenstr. 110
D – 10115 Berlin
Germany
E-Mail: wuensche@physik.hu-berlin.de

No. 849

Berlin 2003

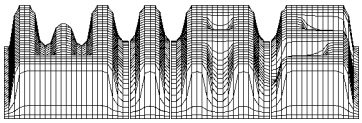

Key words and phrases. semiconductor laser, optical feedback, pulsations.

1999 Physics and Astronomy Classification Scheme. 42.65.Sf.

Edited by
Weierstraß-Institut für Angewandte Analysis und Stochastik (WIAS)
Mohrenstraße 39
D — 10117 Berlin
Germany

Fax: + 49 30 2044975
E-Mail: preprint@wias-berlin.de
World Wide Web: http://www.wias-berlin.de/

Abstract

We describe the basic ideas behind the concept of DFB-lasers with short optical feedback for the generation of high-frequency self-pulsations (SPs) and show the theoretical background describing realized devices. It is predicted by theory that the SP frequency increases with increasing feedback strength. To provide evidence for this we propose a novel device design which employs an amplifier section in the integrated feedback cavity of a DFB-laser. We present results from numerical simulations and experiments. It has been shown experimentally that a continuous tuning of the SP frequency from 12 to 45GHz can be adjusted via the control of the feedback strength. The numerical simulations which are in good accordance with experimental investigations give an explanation for a self stabilizing effect of the SPs due to the additional carrier dynamic in the integrated feedback cavity.

1 Introduction

High repetition frequency pulsed sources are required for a number of signal processing applications in optical time division multiplexed (OTDM) transmission. A key use of such sources is optical clock recovery, which is an essential function that is required to achieve demultiplexing, add-drop multiplexing in the time domain and 3R regeneration [1, 2]. For this purpose monolithically integrated semiconductor devices are attractive because of their compactness, low power consumption and reliability. The tuneability of the generated pulsation frequency in these devices is an important aspect since it lowers the demands on precise technological control of critical design parameters (e.g. cavity lengths) and it offers the possibility to provide a device at various pulse repetition frequencies.

One favoured option for pulse sources is mode-locked semiconductor lasers. The pulsation rate is proportional to the round trip time of the resonator, which can be varied with the aid of a refractive index induced change of the effective length. However, since the current-controlled change of their effective length is very small, the tuning range of the generated pulse repetition frequency is correspondingly limited [3]. A second class of devices offering high frequency generation is semiconductor lasers consisting of two DFB sections and an integrated phase tuning section. They have been used to provide tuneable self-pulsations due to dispersive Q-switching (DQS) with pulsation rates in the order of the relaxation oscillations [4], as well as mode-beating pulsations in dual-mode lasers with two highly-pumped DFB sections [5]. These devices are driven by direct current, which eliminates the cost and complexity of RF power supplies.

In contrast to solutions reported previously, this paper presents an investigation of a resonator design that is novel in the context of promoting self-pulsations (SPs). It consists of one DFB section with a compound cavity to allow the control of the feedback strength. The device, which is a semiconductor laser diode that is subject to delayed optical feedback, has been studied extensively in the literature in other contexts. It is well known that effects such as stable laser operation, excitability [6], chaotic behaviour [7] and SPs [8] can be observed in such laser systems. However, the work presented here focuses on fast SPs because of their applicability in optical signal processing.

The paper is structured as follows. The operating principles of DFB lasers with short optical feedback sections are presented with reference to the Lang-Kobayashi approach in Section II. We propose a novel device design as a consequence of the theoretically predicted dependency of the SP frequency on the feedback strength. The device allows the adjustment of the feedback strength of a DFB due to an amplifier section which is allocated in its integrated feedback cavity. Section III discusses experimental results on fabricated devices while in Section IV a numerical simulation tool is introduced. A verification of our understanding of the device concept by numerical simulations is presented in section V.

2 Self-Pulsations in Lasers with short optical Feedback

We consider a semiconductor laser subject to optical feedback from a short external cavity (EC) of length L_{EC}, as depicted in Fig. 1a. The feedback can be characterised by the relation

$$E_{in}(t) = Ke^{i\phi} \cdot E_{out}(t-\tau) \tag{1}$$

where the real numbers K and ϕ are the strength and phase of the feedback, respectively. The delay time τ is determined by the length of the external cavity $\tau = 2L_{\mathrm{EC}}/v_g$, in which v_g is the group velocity. Using the Lang-Kobayashi (LK) model [9], it has been shown theoretically [10, 11, 12], that such laser systems can generate high frequency pulsations (TP pulsations) due to the coexistence of two external cavity modes having the same threshold gain. A beating of these modes results in high frequency pulsations where the pulse rate is determined by the frequency difference of two lasing modes. This happens even though one of them is dynamically unstable. In particular, it has been shown that the frequency separation f of the beating mode pair increases with the feedback strength according to the relation (see [13] for details)

$$K = K_0 \cdot \left| \frac{\pi \cdot f \cdot \tau}{\sin(\pi \cdot f \cdot \tau)} \right|; \qquad K_0 = \frac{1}{2C_f} \frac{L_{\mathrm{DFB}}}{L_{\mathrm{EC}}}. \tag{2}$$

The factor K_0 is determined by the fraction of the effective lengths of DFB and EC and by the feedback sensitivity C_f of the DFB according to [14]. K_0 represents the minimum feedback strength which is required for the appearance of TP pulsations.

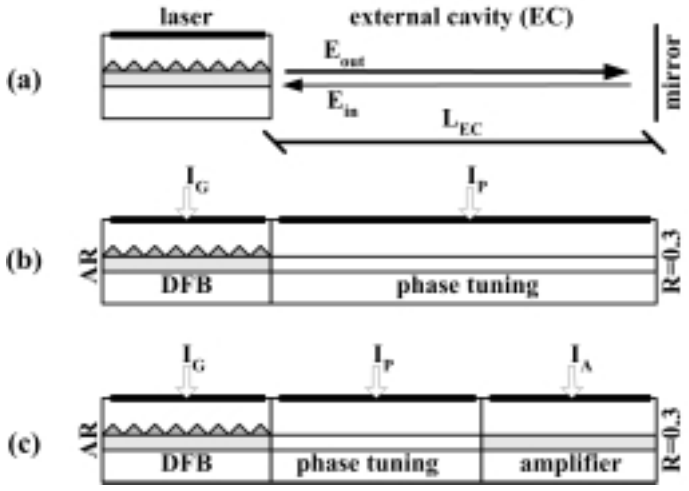

Figure 1: Scheme of the DFB lasers that are designed to produce self pulsations (a) cavity that is subject to optical feedback (general concept) (b) DFB laser with passive feedback (passive feedback laser=PFL)(c) DFB laser with amplified feedback (active feedback laser=AFL)

An important consequence of Eq. (2) is that a high feedback strength $K \gg K_0$ is required to achieve high frequencies $f \to 1/\tau$. Given this feedback, TP pulsations can be achieved only within a rather small interval of the feedback phase φ. This sensitive dependence on parameters requires a careful adjustment of the optical length of the cavity and makes it difficult to observe these pulsations in experiment.

Ref. [6] presents studies of real devices of the type depicted in Fig. 1(b) in which a single laser with distributed feedback is supplemented by a passive section with a cleaved facet as its end mirror. For these devices, known as passive feedback lasers (PFLs), two limitations in terms of high frequency generation were identified. Firstly, the feedback strength in the realized devices is low due to optical losses which arise in the integrated feedback cavity. The losses are due to the active-passive interface, scattering losses in the passive section and a reflectivity at the rear facet which is determined by the refractive index discontinuity between the semiconductor waveguide and air (≈ 0.3). We therefore obtained SP frequencies which were below 20 GHz. One possibility to overcome this limitation is the use of an appropriate high reflection coating. However a remaining problem with PFLs is the absence of control of the feedback strength, which results in a limited control of the SP frequency.

We have therefore concluded that there is a need to integrate an amplifier section into the feedback cavity, as shown in Fig. 1(c), to reach higher feedback values and hence higher frequencies [15]. The proposed active feedback laser (AFL) enables us to control the feedback strength via the current applied in the amplifier section.

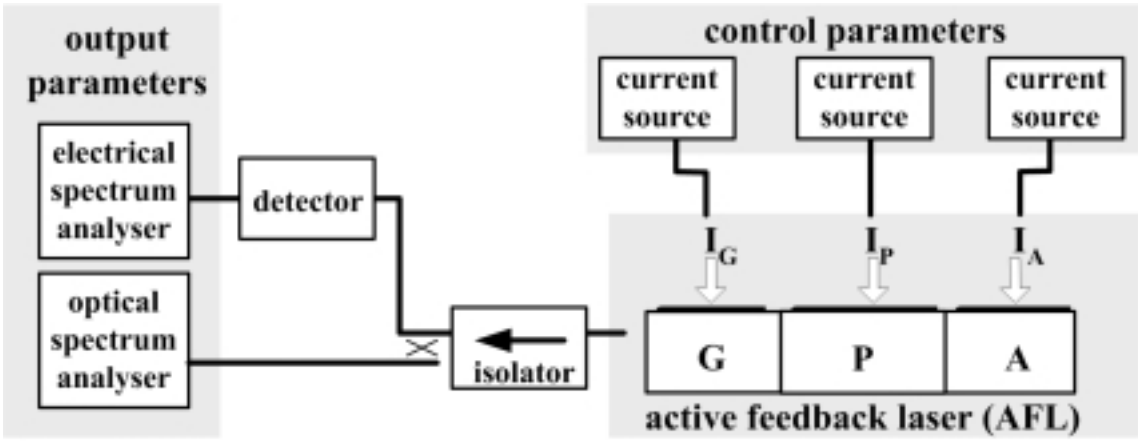

Figure 2: Measurement setup for experimental characterization of the AFL.

3 Active Feedback Laser: Device Preparation and Experiment

The idea of the AFL has been verified by experiments. A first device that we fabricated for this purpose is depicted in Fig. 1(c). It consists of a DFB, a phase section, and an amplifier section with lengths of 200 μm, 350 μm and 250 μm, respectively. The AFL that we analyzed was anti-reflection (AR) coated on the DFB facet with a remaining power reflectivity of 10^{-4}. The back facets are as cleaved, resulting in a power reflectivity of ≈ 0.3. The device is based on InGaAsP-InP material system and the optical wave is guided by a ridge waveguide structure. The active bulk layer ($\lambda_{g,G} = 1.55$ μm) of the DFB section and of the amplifier section is embedded into an asymmetric 1.18 μm / 1.3 μm InGaAsP optical waveguide. The DFB section has an index coupled grating without phase shifts. To prevent mode switching between the two stop-band sides of the DFB we chose a coupling coefficient of κ=130 cm^{-1}. The short wavelength mode is supported by the resulting longitudinal spatial hole burning. Integrated twin-guide coupling was applied between the active and passive sections. For fabrication of the passive section the upper 1.18 μm waveguide and the active layer was removed by dry etching leading to a residual $\lambda_{g,P} = 1.3\,\mu$m waveguide. A density change of the induced carriers in this section leads to a change of the refractive index at 1.55 μm. The refractive index determines the effective length and hence the phase condition ϕ_P. The current I_P can therefore be used for the phase tuning, which is necessary to obtain the TP pulsations. Details of the slightly nonlinear relation between effective refractive index and I_P can be found, e.g. in Ref. [16]. In our present devices, up to 4 phase periods are observed when increasing I_P up to 50 mA. The measurement setup which was used for characterization of the fabricated AFL is depicted in Fig.2. The control parameters are three dc currents. The output of the DFB-section is coupled into an optical fiber followed by an isolator to suppress distorting reflections arising from the measurement setup.

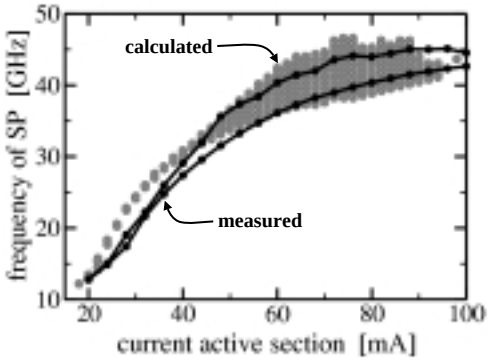

Figure 3: Dependence of SP frequency on the current I_A injected into the amplifier section of the AFL. Solid lines: minimal and maximal measured frequencies. Shadowed area: calculated. At every I_A, the phase has been varied over a full period, yielding a range of frequencies given by separation of solid lines and the width of the shadowed area in case of experiment and calculation, respectively.

An optical spectrum analyzer was used to measure the amplitudes and wavelengths of the lasing modes. The optical signal of the AFL is also converted with a fast photodiode and recorded with an electrical spectrum analyzer, allowing us to detect SPs with frequencies up to 50 GHz. The DFB-current I_G and the temperature of the device were kept constant at 80 mA and 20 °C, respectively throughout the experiments to analyze solely the impact of the parameters controlling the feedback strength and the phase in the integrated feedback cavity.

Fig. 3 is a plot of the frequencies of the SPs against the current of the amplifier section and it shows that the frequencies generally increase with rising I_A. A frequency tuning range from 12 to 45 GHz has been experimentally obtained. SPs with frequencies above 12 GHz could be generated for all amplifier currents above 20 mA if the phase current is adjusted appropriately. This experimental result is in agreement with the assumption that the amplifier section just increases the feedback level and confirms the tunability of the SP frequency by I_A. An additional very advantageous effect comes into view in Fig. 3. At higher amplifier currents, the phase current has a considerable influence on the frequency. This phenomenon improves the tunability of the SP frequency. A continuous tuning of the frequency from 15 GHz up to 45 GHz could be achieved by using both currents. A different view of the same effects is given in Fig. 4, showing the variations of the measured SP frequencies with phase. As mentioned before, four phase periods are observed when increasing I_P from 0 to 50 mA. Two different amplifier currents are considered, being representative for the low- and high-current regimes in Fig. 3, respectively. The lower trace was measured close to the transparency pump level of the amplifier section, which therefore can be considered as passive. Accordingly, we find SP only within a small phase interval, as known from lasers with passive feedback (PFL). In the high-current regime (see upper trace in Fig. 4), the situation is completely different. SPs appear over

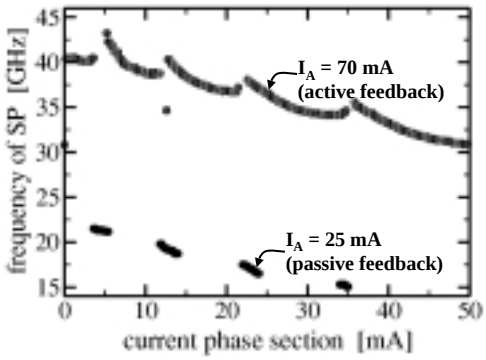

Figure 4: Measured frequencies of SPs obtained when tuning the phase current. The current at the DFB-section was kept constant at 80 mA. The current at the amplifier section was 25 mA (black points) and 70 mA (shaded points) for representation of the PFL and AFL, respectively.

a huge range of one phase period and the frequency varies over a wider range as already stated above. Such behavior is very favorable for applications since it lowers demands on a precise current control. Moreover, it indicates that the impact of the amplifier section results not only in a higher feedback but also in a self-stabilization of the SP which will be investigated in the following sections.

Summarizing so far, the fabricated AFL devices exhibit the expected high-frequency SPs tunable by the amplifier current up to 45 GHz. Additionally, the phase range in which fast SPs occur increases with increasing amplifier current. The effect results in a wide tunability of the frequency by means of the phase current.

4 Description and Test of a Numerical Simulation Tool

We have performed simulations in order to provide a deeper understanding of the described observations. The Lang-Kobayashi approach was not directly applicable because the carrier density n_A of the amplifier section comes into play as an additional dynamic variable. We therefore used a model that is based on the so called travelling wave equations (TWE) [17, 18, 19]. They describe the spatio-temporal evolution of two counter-propagating optical fields with slowly varying amplitudes $E(z,t) = (E^+, E^-)$ along the longitudinal axis of the device ($z \in [0, L]$). These optical amplitudes are coupled to local polarization functions $p(z,t) = (p^+, p^-)$ and

carrier densities $n(z,t)$ within the DFB- and amplifier sections:

$$\begin{aligned}
\frac{\partial}{\partial t}E^{\pm} &= v_g\Big(\mp\frac{\partial}{\partial z} - i\beta - \frac{\alpha}{2}\Big)E^{\pm} - iv_g\kappa E^{\mp};\\
\frac{\partial}{\partial t}p^{\pm} &= \bar{\gamma}(E^{\pm} - p^{\pm}) + i\bar{\omega}p^{\pm};\\
\frac{\partial}{\partial t}n &= J - R(n) - 2v_g\Im m[E^*\beta E].
\end{aligned} \tag{3}$$

The boundary conditions at the facets are $E^+(0,t) = r_0E^-(0,t)$ and $E^-(L,t) = r_LE^+(L,t)$.

The active waveguide within the DFB and amplifier sections is modelled by the propagation term

$$\beta E^{\pm} = \Big(\delta + \frac{g}{2}(i+\alpha_H)\Big)E^{\pm} + i\frac{\bar{g}}{2}(p^{\pm} - E^{\pm}) \tag{4}$$

containing the maximum gain with nonlinear saturation

$$g(n,|E|^2) = \frac{g'(n-n_t)}{1+\varepsilon|E|^2}. \tag{5}$$

By proper normalization, $|E(z,t)|^2 = |E^+|^2 + |E^-|^2$ is a local photon density (local power at z divided by the global constant $\hbar\omega_0 v_g A_{AZ}$). The last term of (4) together with the oscillator model in Equ. (3) for the polarization represents the time domain description of the dispersive contribution

$$\Delta\beta_{disp}(\omega) = i\frac{\bar{g}}{2}\left(\frac{\bar{\gamma}^2 - i\bar{\gamma}(\omega-\bar{\omega})}{(\omega-\bar{\omega})^2+\bar{\gamma}^2} - 1\right) \tag{6}$$

to the waveguide propagation constant [17]. It corresponds to a Lorentzian gain dispersion (magnitude $\bar{g}$, width $2\bar{\gamma}$, position of maximum $\bar{\omega}$) together with its refractive index contribution according to the Kramers-Kronig relation.

The recombination $R(n)$ and the inhomogeneous injection $J(z,t)$ in the carrier rate equation (3) are given by

$$\begin{aligned}
R(n) &= An + Bn^2 + Cn^3,\\
J(z,t) &= \frac{I}{eV} - \frac{U_F'}{eVR_s}(n(z,t) - \bar{n}(t)),
\end{aligned} \tag{7}$$

where $\bar{n}(t)$ denotes a spatial average of the carrier density $n(z,t)$ over the corresponding laser section.

In the $\lambda_{g,P} = 1.3$ μm phase section, the injected carriers do not couple to the $\lambda_{g,G} = 1.55$ μm laser light, but only cause a refractive index change. For simplicity, we disregard carrier and polarization equations completely, express the propagation constant as

$$\beta = -\frac{\phi_P}{2L_P} \qquad (z \in \text{phase section}), \tag{8}$$

and treat the contribution ϕ_P of this section to the feedback phase as a tunable parameter.

The numerical calculations were performed with the program suite LDSL (abbreviation for Longitudinal Dynamics in Semiconductor Lasers). Besides solving the system of TWE equations in time domain, this suite provides powerful tools to analyze the results from different points of view. The appearance of SPs was detected from the Fourier transform of one output intensity, yielding also the pulsation frequencies. As in the experiments, we fixed I_G and varied I_A in our simulations. Other parameters are given in Table 5.

Calculated frequencies of the SPs are depicted together with the experimentally obtained data in Fig. 3, from which it can be seen that there is a good agreement for all amplifier currents. There are two key similarities between the modelling and the experimental data. The first is the increase in SP frequency with increasing current I_A in the amplifier section. The second is the rapid increase in tuneability with increasing I_A and this is due to the passive phase ϕ_P. From this very satisfactory overall agreement we draw the conclusion that the calculated device is a good model of the fabricated laser and can be applied to obtain a deeper understanding of the system.

5 Numerical Simulation: Impact of Amplifier Section on Fast Self-Pulsations

For a better understanding of the observed influence of ϕ_P on the SP frequency, one has to realize that the internal state of the amplifier section is not fixed by the injection current I_A but it responds to changes of ϕ_P. The major effect in this context is the variation of the average carrier density n_A of the amplifier depicted in Fig. 5. This variation transforms into changes of the average feedback strength and phase according to the relations

$$\begin{aligned} K &= |r_L| \exp\left(-\alpha_P L_P\right) \exp\left((g_A(n_A) - \alpha_A) L_A\right), \\ \phi &= \arg(r_L) + \phi_P - \alpha_H g_A(n_A) L_A, \end{aligned} \tag{9}$$

with the mean amplifier gain $g_A(n_A)$. The corresponding variations of K and ϕ over one period of ϕ_P are also plotted in Fig. 5. To clarify their impact on the frequencies, Fig. 6 shows the calculated data of Fig. 3 with now using $K(n_A)$ as abscissa instead of I_A. A clear reduction of the frequency scatter is obtained. To understand the residual frequency band, we have repeated the calculations for a series of equivalent PFLs. These PFLs differ from the AFLs by only two parameters. First, we have set I_A to the transparency value. This situation was carefully adjusted to keep n_A at the gain transparency, which results in a passive behavior of the amplifier section. Second, we have used the absorption coefficient α_A of the amplifier section to vary the feedback strength. The resulting graph of the SP frequencies vs. K in Fig. 6 is very close to that of the AFL, which is a strong evidence that the AFL

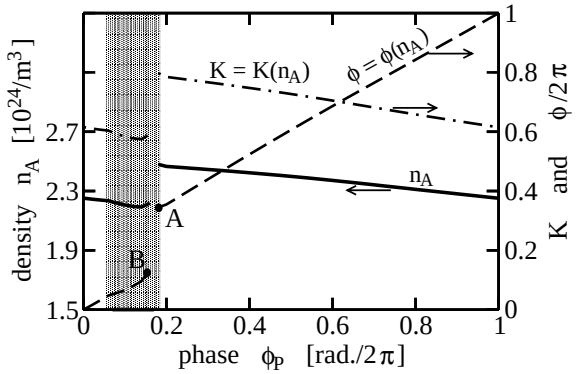

Figure 5: Variation of averaged carrier density $\langle n_A \rangle$ in the amplifier section as well as magnitude K and phase ϕ of the feedback in an AFL at $I_A = 70$ mA versus the phase shift ϕ_p introduced by the phase section. The shaded area indicates the phase interval where SP of TP type were observed.

behaves like a laser with an equivalent passive feedback. Fig. 6 also contains a curve representing the simple relation (2). A good agreement over a wide range of K is obtained, supporting the interpretation of the SP in terms of two beating modes. Deviations appear only for very small and large values of K. At high K the LK-model is not valid. At small K, the numerical simulations yielded SPs of the DQS type (undamped relaxation oscillations), which of course are not described by the analytic mode-beating condition (2). They have, however, been predicted by numerical bifurcation analysis of the LK-model [13] as well as of a TWE-model [20]. Moreover, frequencies below 10GHz are present also in the range of medium and high K. They appear only in a small range of ϕ_P (in of the shaded area of Fig. 5) and will be studied elsewhere.

The good agreement of Equ. (2) to the numerical data was obtained by using $K_0 = 0.125$ and $\tau = 23.2$ps. The insertion of the C_f-value of Favre [14] into Equ. (2) yields $K_0 \approx 0.2$. This is a reasonable agreement in view of the neglect of spatial hole burning by Favre. The delay time $\tau = 23.2$ corresponds to a feedback length $L_P + L_A \approx 900\mu$m, being distinctly larger than the 600μm geometrical length. The difference cannot be explained by the uncertainties of the group refractive indexes. Instead, we believe it is connected with the spatial extension of the fields over the whole DFB section, not taken into account by the LK model. A final clarification of this item would require a deeper investigation of the relations between the TW and LK models, which is beyond the scope of this paper.

The influence of n_A on the feedback strength discussed so far explains accurately the variation of frequencies with phase in terms of an equivalent PFL. Now we regard the phase ranges with showing self-pulsations already discussed in connection with Fig. 4. Why is this range small in the PFL-regime of operation but becomes huge for higher amplifier currents? Fig. 7 gives an answer to this question. Here the calculated data for the AFL and the PFL are plotted separately in the $K - \phi$

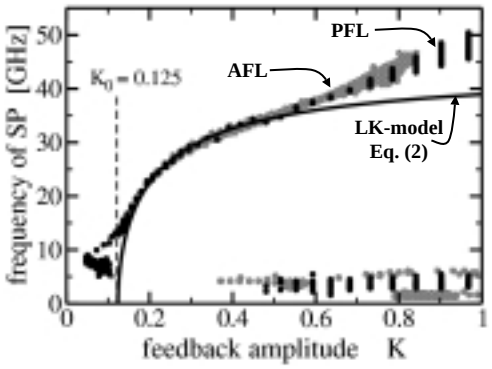

Figure 6: Frequency of SP versus the feedback amplitude K. Shaded points: AFL, the same numerical data as drawn vs. I_A in Fig. 3. Black points: a corresponding PFL with different feedback K. Solid line: fit to Eq. (2) with $K_0 = 0.125$ and $\tau = 23.2ps$ which corresponds to a feedback length of $L = 900\mu m$.

plane. The shadowed area represents the points (K, ϕ) with high-frequency SPs. Obviously both SP regions nearly coincide, indicating again that an AFL at a given operation point behaves similar to the equivalent PFL. Nevertheless, a PFL and an AFL behave very different when tuning only ϕ_P (resp. I_P) while keeping all other parameters constant. A PFL follows the line K =const., $\phi = \phi_P$ and the SP region is crossed horizontally, filling only a small part of one period. In an AFL, we have instead I_A =const. and K falls with ϕ_P within the SP region due to the readjustment of n_A (cf. Fig. 5). At the same time, ϕ varies less than ϕ_P by the same reason. Both effects together tilt the tuning line I_A =const. (full points) nearly along the SP region. Moreover, this line does not overlap the full period of ϕ. It ends just after leaving the SP region. At this point the sudden jump of n_A kicks the system back to the start of the tuning line at the opposite border of the SP region. It is this self adjustment of the feedback parameters via the mean amplifier carrier densities which allows the observation of robust high frequency SPs in large areas of the control parameter plane.

6 Conclusions

A theoretical and experimental investigation of the generation of high-frequency SPs by DFB-laser with a short optical feedback is reported in this paper. It was found that the SP frequency increases with the strength of the light which is fed back into the DFB-laser. SP frequencies in the range of 20GHz were achieved for lasers incorporating a passive feedback section (PFL). Moreover, a very critical behavior in terms of the phase of the light fed back was identified which is in good agreement

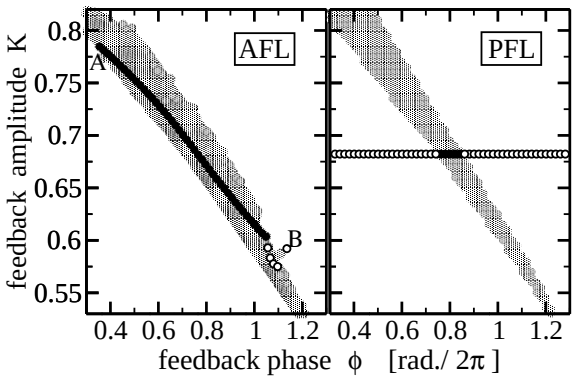

Figure 7: Regions of self-pulsations SPs in a part of the (K, ϕ)-plane. Shaded area: AFL with different I_A and ϕ_P; Solid black points: AFL with $I_A = 70$ mA and different ϕ_P (same data as drawn in Fig. 4). Area separated by solid lines: PFL at K and ϕ_P varied independently of each other; open points: PFL for some fixed K and varied ϕ_P.

	explanation	values			unit
		G	P	A	
κ	coupling coefficients	130	0	0	cm^{-1}
L	section lengths	200	350	250	μm
A_{AZ}	cross sectional area of active zone	0.45		0.45	μm^2
c/v_g	group velocity index	3.8	3.8	3.8	
g'	effective differential gain	9		9	10^{-17} cm^2
ε	nonlinear gain compression	3		3	10^{-18} cm^3
n_{tr}	transparency carrier density	1		1	10^{18} cm^{-3}
α_H	Henry factor	-4		-4	
α	internal absorption	25	20	25	cm^{-1}
δ	frequency detuning	402.7			cm^{-1}
A	recombination coefficient	1		1	10^9 s^{-1}
B	recombination coefficient	1		1	10^{-10} cm^3 s^{-1}
C	recombination coefficient	1		1	10^{-28} cm^6 s^{-1}
R_s	series resistance	2.5		2.5	Ω
U'_F	differential Fermi level separation	6		6	10^{-20} V cm^3
$\bar{g}$	Lorentzian heigth	150	0	150	cm^{-1}
$\bar{\gamma}$	Lorentzian half width	23.5		23.5	ps^{-1}
$\bar{\omega}$	Lorentzian central frequency	4.7		4.7	ps^{-1}
	reflectivity coefficients at facets	r_0=0		r_L=$\sqrt{0.3}$	

Table 1: Parameter values used for the DFB gain (G), phase tuning (P), and amplifier (A) sections.

with analytical models presented elsewhere [13]. The need for an additional amplifier section in the integrated feedback cavity was identified as a consequence of speed and tuning limitations of the PFLs. In the AFL the additional amplifier enables compensation of the optical losses and to control the feedback strength. A fabricated device served to experimentally demonstrate two facts. First, a wide tuning range of the SP frequency can be obtained by control of the amplifier current and therefore controlling the feedback strength. Second, the areas where fast SPs occur increase with increasing amplifier current, indicating that the additional carrier dynamic in the added amplifier sections results in a self adjusting effect of the feedback amplitude and phase. To provide a deeper understanding of the experimentally obtained results a travelling wave model was used to study the experimental data. The modelling results demonstrate clearly that if the carrier density in the active feedback is high the feedback phase and amplitude settle dynamically to a situation where the condition for high frequency pulsations are satisfied. This self-adjusting effect is based on the additional changes of carrier density which acts in the integrated feedback cavity of the device investigated. Due to the self adjustment of feedback amplitude and phase the AFL is more stable for generation of high frequency pulsations than the PFL.

We believe that the results that we report provide a deeper understanding of self-pulsation phenomena in multisection DFB lasers, which will ultimately be important in applications such as clock recovery in high capacity communications.

Acknowledgments

Part of the experimental work has been performed within the framework of the Research Partner Program of Alcatel. This work was supported by Deutsche Forschungsgemeinschaft (DFG). Useful comments and suggestions by P. Urquhart and D. Hoffmann are appreciated.

References

[1] M. Saruwatari *All-Optical Signal Processing for Terabit/Second Optical Transmission* IEEE J. on Sel. Top. Quantum Electron., vol. **6**, no. 6, pp. 1363-1374, 2000.

[2] P. Brindel, B. Dany, D. Rouvillain, B. Lavigne, P. Guerber, E. Balmefrezol, O. Leclerc *All-Optical Signal Regenerators for Ultra-High Bit-Rate Transmission Systems*, IEICE Transactions on Electronics, vol. E85-C, no. 1, pp. 126-134, Jan. 2002.

[3] I. Ogura, H. Kurita, T. Sasaki, H. Yamada, H. Yokoyama *A precisely frequency-controlled mode-locked laser diode for all-optical clock extaction at 40GHz SDH frequency*, SPIE July 1999, Denver, Colorado, vol. 3795.

[4] M. Radziunas, H.-J. Wünsche, B. Sartorius, O. Brox, D. Hoffmann, K. Schneider, and D. Marcenac , *Modeling Self-Pulsating DFB Lasers with an Integrated Phase Tuning Section*, *IEEE J. Quantum Electron.*, vol. **36**, No. **9**, pp. 1026-35, 2000.

[5] M. Möhrle, B. Sartorius, C. Bornholdt, S. Bauer, O. Brox, A. Sigmund, R. Steingrüber, M. Radziunas, H.-J. Wünsche *Detuned Grating Multisection-RW-DFB Lasers for High Speed Optical Signal Processing*, IEEE J. on Sel. Top. Quantum Electron. , vol. **7**, pp. 217-223, 2001.

[6] H.-J.Wünsche, O.Brox, M.Radziunas and F.Henneberger, *Excitability of a Semiconductor Laser by a Two-Mode Homoclinic Bifurcation*, Phys.Rev.Lett. 88,f 023901 (2002)

[7] J. Mørk, B. Tromborg, and J. Mark , *Chaos in Semiconductor Lasers with Optical Feedback: Theory and Experiment*, *IEEE J. Quantum Electron.*, vol. **28**, pp. 93-108, Jan. 1992.

[8] B. Sartorius, M. Möhrle, S. Reichenbacher, H. Preier, H.-J. Wünsche, and U. Bandelow, *Dispersive self Q-switching in self-pulsating DFB lasers*, *IEEE J. Quantum Electron.*, vol.**33**, pp. 211-218, 1997.

[9] R. Lang, K. Kobayashi, *External Optical Feedback Effects on Semiconductor Injection Laser Properties*, *IEEE J. Quantum Electron.*, **16**, pp. 347-355, 1980.

[10] A. Tager, *Mode Competition and Mode Locking in Compound Cavity Semiconductor Lasers*, *IEEE Photonics Technology Letters* , vol. **6**, no. 2, pp. 164-166, 1994.

[11] A. Tager and K. Petermann, *High Frequency Oscillations and Self-Mode Locking in Short External-Cavity Laser Diodes*, *IEEE J. of Quantum Electronics* , vol. **30**, pp. 1553-1561, 1994.

[12] T. Erneux , F. Rogister, A. Gavrielides, V. Kovanis *Bifurcations to mixed external cavity mode solutions for semiconductor lasers subject to optical feedback*, *Opt. Comm.* , **183**, pp. 476-477, 2000.

[13] M. Wolfrum, D. Turaev, *Instabilities of lasers with moderately delayed feedback*, *Optics Comm.* 212/1-3, pp. 127-138, 2002.

[14] F. Favre *Theoretical Analysis of External Optical Feedback on DFB Semiconductor Lasers*, *IEEE J. Quantum Electron.*, vol. **QE-23**, no.1, pp. 81-88, 1987.

[15] S. Bauer, O. Brox, J. Kreissl, G. Sahin, B. Sartorius *Optical microwave source*, *Electronic Letters*, **38**, March, 2002.

[16] U. Bandelow, H.-J. Wünsche, B. Sartorius and M. Möhrle *Dispersive self-Q-switching in DFB lasers: Theory versus experiment*, *IEEE J. Selected Topics in Quantum Electronics*, vol. **3**, pp. 270-278, 1997.

[17] U. Bandelow, M. Radziunas, J. Sieber, M. Wolfrum, *Impact of Gain Dispersion on the Spatio-Temporal Dynamics of Multisection Lasers*, *IEEE J. Quantum Electron.*, **37**, pp. 183-188, 2001.

[18] H.J. Wünsche, U. Bandelow, H. Wenzel and D. Marcenac, *Self pulsations by mode degeneracy in two-section DFB lasers*, *SPIE Proceedings Series*, **2399**, pp. 195-206, 1995.

[19] U. Feiste, *Optimization of Modulation Bandwidth in DBR Lasers with Detuned Bragg Reflectors*, *IEEE J. Quantum Electron.*, vol.**34**, no.12, pp. 2371-2379, 1998.

[20] J. Sieber *Numerical Bifurcation Analysis for Multi-Section Semiconductor Lasers*, SIAM J. on Appl. Dyn. Sys., Vol. 1, No. 2, pp. 248-270, 2002.